Light-induced electronic non-equilibrium in plasmonic particles

Mordechai Kornbluth, Abraham Nitzan, and Tamar Seideman

Citation: J. Chem. Phys. **138**, 174707 (2013); doi: 10.1063/1.4802000
View online: http://dx.doi.org/10.1063/1.4802000
View Table of Contents: http://jcp.aip.org/resource/1/JCPSA6/v138/i17
Published by the American Institute of Physics.

Light-induced electronic non-equilibrium in plasmonic particles

Mordechai Kornbluth,[1] Abraham Nitzan,[2,a)] and Tamar Seideman[1,b)]
[1]*Department of Chemistry, Northwestern University, Evanston, Illinois 60208, USA*
[2]*Department of Chemistry, Tel Aviv University, Tel Aviv 69978, Israel*

(Received 30 December 2012; accepted 8 March 2013; published online 6 May 2013)

We consider the transient non-equilibrium electronic distribution that is created in a metal nanoparticle upon plasmon excitation. Following light absorption, the created plasmons decohere within a few femtoseconds, producing uncorrelated electron-hole pairs. The corresponding non-thermal electronic distribution evolves in response to the photo-exciting pulse and to subsequent relaxation processes. First, on the femtosecond timescale, the electronic subsystem relaxes to a Fermi-Dirac distribution characterized by an electronic temperature. Next, within picoseconds, thermalization with the underlying lattice phonons leads to a hot particle in internal equilibrium that subsequently equilibrates with the environment. Here we focus on the early stage of this multistep relaxation process, and on the properties of the ensuing non-equilibrium electronic distribution. We consider the form of this distribution as derived from the balance between the optical absorption and the subsequent relaxation processes, and discuss its implication for (a) heating of illuminated plasmonic particles, (b) the possibility to optically induce current in junctions, and (c) the prospect for experimental observation of such light-driven transport phenomena. © *2013 AIP Publishing LLC*. [http://dx.doi.org/10.1063/1.4802000]

I. INTRODUCTION

The optical excitation of noble metal nanoparticles triggers a sequence of photophysical events that typically vary widely in time- and length-scales, starting with ultrafast decoherence of the optically formed plasmon (taking place at ∼10 fs timescales), and followed by electron-electron scattering (100 fs), electron-phonon coupling (1-5 ps), and finally, relatively slow heat dissipation processes (10-100 ps). Similar to the effect of noble metal nanostructures on an incident electromagnetic radiation, which manifests itself as wavelength-sensitive local enhancement of the incident energy, heating affected by the incident radiation on such structures has been the topic of intensive experimental and theoretical research in recent years. This effort has been fueled both by the fascinating physics involved in the fundamental sequence of events leading to conversion of optical energy into heat, and by a large variety of applications of optical heating of nanoparticles, in areas such as nanoscale catalysis,[1,2] magnetism,[3] microfluidics,[4–7] phononics,[8,9] medicine,[10–15] imaging and spectroscopy,[16–19] information storage[20] and processing,[21,22] and nanoscale patterning.[1]

In these traditional applications, the optical excitation of nanoparticles serves as a spatially-localized heating mechanism. In this paper, we address another consequence of this excitation—the transient, strongly non-equilibrium distribution of carriers established by the incident radiation that may modify the conductance properties of metallic nanojunctions and may provide new means of driving chemical events.

Although the physics of optical heating of metal surfaces and thin metal films has much in common with that of optical heating of metal nanoparticles, nanoparticles have an advantage as controlled nanosources of heat and a route to designing and measuring temperature distributions at sub-diffraction length-scales. First, the plasmon resonance mechanism, characteristic of metal nanoparticles subject to light, leads to large cross-sections for light absorption, thus making metal nanoparticles excellent converters of optical energy into heat. Second, several decades of experience have perfected the fabrication and characterization of noble-metal nanoparticles. Hence their optical and thermal properties are controllable and can be systematically varied by tuning their shape, size, relative arrangement, and composition.

The qualitative physics underlying the interaction of laser fields with metal nanoparticles at their plasmon resonance frequency is well understood.[23,24] The incident light excites a dipolar oscillation of the conduction electrons—a dipolar plasmon, which rapidly dephases to become a distribution of uncorrelated electron-hole excitations. The corresponding dephasing time depends on the size of the particle and contributes to the linewidth of the plasmon resonance. For small particles, this process is dominated by electron-surface scattering with additional contributions of impurity scattering and electron-electron interactions. In large particles, radiation damping becomes an important factor in the plasmon line-broadening. Light absorption with subsequent dephasing thus results in deposition of energy into the electron distribution, creating excited electron-hole pairs that are spread over different levels in the conduction band. This excited electronic distribution rapidly (on a few 100 fs timescale) equilibrates within itself, giving rise to a hot electronic temperature that deviates strongly from the phonon temperature. In the process, memory of the electron excitation dynamics is entirely lost. The subsequent equilibration of the hot electrons with the phonons, on a picosecond timescale, is often described within

a)nitzan@post.tau.ac.il
b)t-seideman@northwestern.edu

a two-temperature model, dating back to the 1957 work of Kaganov *et al*.[25] (see also Ref. 26). Here, the rate of change of the electronic and phonon temperatures is described by a pair of coupled differential equations that is determined by the electron-phonon coupling strength and by the electronic and lattice heat capacities. Finally, once equilibrium has been established between the electrons and the lattice, the hot particle equilibrates with its environment, on a >10 ps timescale, via heat transfer across the interface between the particle and its surroundings and heat diffusion in the medium. (Clearly, this convenient partitioning of the relaxation into sequential non-overlapping events is only approximate and not entirely general.)

From an experimental perspective, the physical processes leading to conversion of optical excitation into heat have been addressed by a combination of different spectroscopic techniques in both energy and time domains. These include spectral broadening measurements, which, in the limit of purely homogeneous broadening, reflect the early dephasing of the plasmon resonance in the metal nanoparticle;[27–29] transient absorption experiments, which provide information about the electron-electron and electron-phonon coupling[30–32] and their dependence on the particle size and shape; time-domain studies of the coherent acoustic vibrations which ensue energy flow out of the electronic subspace and into the lattice on a picosecond timescales;[33–35] as well as transient absorption and time-resolved X-ray measurements of hot particle cooling due to interface conductance and heat dissipation to the environment.[36–38] Recent reviews of this large and diverse body of research can be found in Refs. 39 and 40.

Numerical studies of the fundamental physics leading to optical heating have been similarly diverse in scope and application. To date, the vast majority of these studies have focused on the longest timescale process, describing the equilibration of the hot nanoparticle with its environment. The early work of Pustovalov,[41] Govorov *et al*.,[42] and Keblinski *et al*.[43] determined the temperature profile at thermal equilibrium by solving the heat conduction equation [see, for instance, Ref. 44] for a hot sphere (or a collection of spheres) embedded in a medium, using either the Joule-Lenz law, or the computed absorption cross section to determine the heat generation rate. These studies illustrated not only heating but also melting of the embedding medium. A similar approach was taken by Bruzzone and Malvaldi,[45] who stressed the importance of accounting for surface effects and for the inhomogeneity of the electromagnetic field in the particle. The more recent research of Baffou *et al*.[46] extended the discrete dipole approximation and Green's dyadic tensor method, often used in calculations of the optical response of nanoparticles, to investigate also their thermodynamic properties, introducing to that end the thermal Green function and a Laplace matrix inversion algorithm. Considering a chain of gold nanospheres in a homogeneous medium on a glass substrate in air, and on a glass substrate in water, the authors determined the temperature spatial profile, exploring the role played by the distance of the interface with the conductive medium in determining the heat release. Considering a gold gap-antenna as an example of a more complex construct, and applying the Green's dyadic tensor method, Baffou[46] found that the temperature profile behaves qualitatively differently from the optical field profile.[46] (See also Ref. 47 and the combined experimental-numerical work of Baffou *et al*.[48]).

Several recent studies of optical heating of nanoparticles were able to directly compare numerical predictions with experimental data. One example is the work of Cole *et al*.[49] who presented experimental and numerical photothermal transduction efficiencies of SiO_2/Au nanoshells, Au_2S/Au nanoshells, and Au nanorods, directly relevant to clinical therapeutic applications. Their results show that particle size plays a dominant role in determining the transduction efficiency, with larger particles being more efficient for both absorption and scattering. In a related study, using a combination of calculations with photocalorimetric experiments in a water droplet containing gold nanoparticles, Richardson *et al*.[50] found that the photoheating mechanism and energy equilibration details depend strongly on the incident laser intensity and the nanoparticle concentration. The recent research of Nedyalkov *et al*.[51] combined ultrashort pulse experiments with the two-temperature heat model and finite-difference time-domain simulations to explore optical local heating of gold nanoparticles on silicon and dielectric surfaces, with a view to applications in therapeutic treatment of living cells.

To the best of our knowledge, the short time carrier dynamics, characterized by a nonequilibrium electronic distribution, which immediately follows the rapid plasmon dephasing process, was not explored on the microscopic level, although interest in this problem for surfaces of bulk metals and more recently in nanoparticles has been substantial, and semiclassical estimates and experimental ramifications have been discussed.[52] This early dynamics and its consequence for the steady state of an illuminated system are relevant to surface photochemistry and photoelectrochemistry,[53,54] to estimates of the electron transfer ("chemical") contribution in surface enhanced Raman scattering, and potentially to future applications of light-triggered metal nanodevices, such as optically driven or optically controlled molecular conduction junctions,[55,56] and emerging, optically driven nanoelectromechanical systems. It is, furthermore, accessible to currently existing and developing ultrashort pulse technology.

Our goal in the present contribution is to complement the previous experimental and numerical research in this field and fill in the gap in our understanding of the basic physics and potential of optical heating of metal nanoparticles by exploring the ultrashort time carrier dynamics ensuing the plasmon dephasing. To that end we derive closed-form expressions for the nonequilibrium electron distribution established by the optical excitation of a general nanoparticle and its time evolution. The theory is applied to derive a closed form expression for a conveniently defined transient "effective temperature" of the hot particle, and to explore the transport properties of light-driven, bias-free molecular conduction junctions. As shown below, the electron distribution function established by the photon absorption can be defined as a sum of two time-dependent components. One is an electronic thermal component described by a Fermi-Dirac distribution with a time-dependent electronic temperature. The second is a transient nonequilibrium component, whose behavior depends on

the properties of the excitation field, and which is expected to have signatures in experimental observables.

In Sec. II we develop a closed-form expression for the electronic nonequilibrium distribution that ensues the rapid decoherence of the light triggered plasmon. In Sec. III we introduce a simple model to describe the time evolution of this electronic distribution, and in Sec. IV we proceed to discuss the consequent evolution of the electronic temperature. Finally, Sec. V applies the model to the problem of light-driven transport via a molecular junction, and the last section concludes with a discussion of avenues for future research.

II. PLASMON-MEDIATED ELECTRONIC NON-EQUILIBRIUM

Our starting point is the assumption that photon absorption by a small metal particle leads to excitation of a plasmon—a collective coherent superposition of electron-hole pairs. Following the creation of a plasmon, this coherent superposition first decoheres, leading to a non-equilibrium single electron distribution. Electronic relaxation may later lead to a modified Fermi-Dirac distribution characterized by an effective electronic temperature. On a longer timescale, electron-phonon energy exchange leads to further relaxation, in which the electronic and nuclear energies are equilibrated. Finally, full thermal relaxation returns the metallic sub-system to the pre-photon-absorption stage. Here we consider the first stage of this process, in which photon absorption creates a plasmon, whose decoherence yields a transient, far-from-equilibrium distribution of electrons.

For definiteness, we place the equilibrium chemical potential of the particles at $\mu = 0$, so that the equilibrium electronic distribution is

$$f_{eq}(\varepsilon) = [e^{\varepsilon\beta_e} + 1]^{-1}, \tag{1}$$

where $\beta_e = (k_B T_e)^{-1}$, k_B being the Boltzmann constant, and T_e is the electronic temperature that may be different (see Sec. IV) from the ambient temperature. Absorption of a photon of energy $\hbar\omega$ creates a superposition of electron-hole pairs, each of which is characterized by two electronic energies ε_e and ε_h, which satisfy $\hbar\omega = \varepsilon_e - \varepsilon_h$. Our input is the absorption lineshape, $L(\omega)$, defined so that if $\dot{n}_I(\omega, t)d\omega$ is the number of photons incident per unit time in the interval between ω and $\omega + d\omega$, then $\dot{n}_A(\omega, t)d\omega = \dot{n}_I(\omega, t)L(\omega)\,d\omega$ is the number of photons absorbed per unit time in that frequency interval. Note that $\dot{n}_I(\omega, t)$ should reflect the local light intensity at time t, including any possible modification by the plasmonic environment. In the present treatment we limit ourselves to the simple case where the pulse duration τ_{pulse} is long relative to the characteristic excitation frequencies. This allows for the approximate description in terms of a pulse envelope function, $I(t)$

$$\dot{n}_I(\omega, t) = n_I(\omega)I(t); \quad \int_{-\infty}^{\infty} dt' I(t') = 1. \tag{2}$$

The absorption lineshape $L(\omega)$ can be experimentally measured or theoretically calculated, and depends on the nanoparticle composition, geometry and environment.

To make a connection with the resulting electronic distribution, we consider the joint probability density for photon absorption, $A(\omega, \varepsilon_e)$, defined such that $A(\omega, \varepsilon_e)d\omega d\varepsilon_e$ is the (joint) probability of photon absorption of frequency between ω and $\omega + d\omega$ *and* excitation of an electron-hole pair at energy $(\varepsilon_e, \varepsilon_e - \hbar\omega)$ between ε_e and $\varepsilon_e + d\varepsilon_e$. This density satisfies

$$\int_{-\infty}^{\infty} A(\omega, \varepsilon_e)d\varepsilon_e = \frac{n_A(\omega)}{N_A} = \frac{n_I(\omega)L(\omega)}{N_A}, \tag{3}$$

where

$$N_A = \int d\omega n_A(\omega) = \int d\omega n_I(\omega)L(\omega) \tag{4}$$

is the total number of absorbed photons (whereas $N_A I(t)$ is the total number of absorbed photons per unit time at time t), which is equal to the number of electron-hole pairs created. The probability $A(\omega, \varepsilon_e)$ is next written in the form

$$A(\omega, \varepsilon_e) = K n_I(\omega) D(\varepsilon_e, \varepsilon_e - \hbar\omega)\rho_p(\varepsilon_e, \varepsilon_e - \hbar\omega), \tag{5}$$

where $D(\varepsilon_f, \varepsilon_i)$ is the squared magnitude of a transition matrix element for the electronic process $\varepsilon_i \to \varepsilon_f$, $\rho_p(\varepsilon_e, \varepsilon_e - \hbar\omega)$ is the population-weighted density of pair states,

$$\rho_p(\varepsilon_1, \varepsilon_0) = \{f(\varepsilon_0)\rho(\varepsilon_0)\} \times \{[1 - f(\varepsilon_1)]\rho(\varepsilon_1)\}, \tag{6}$$

$\rho(\varepsilon)$ being the density of single electron states at energy ε, and K is a normalization constant that ensures the equality $\int_{-\infty}^{\infty} d\varepsilon_e \int_0^{\infty} d\omega A(\omega, \varepsilon_e) = 1$. In terms of $A(\omega, \varepsilon_e)$, the numbers of electrons and holes created by the excitation process in the energy range $\varepsilon ... \varepsilon + d\varepsilon$ are $N_e(\varepsilon)d\varepsilon$ and $N_h(\varepsilon)d\varepsilon$, respectively, where

$$N_e(\varepsilon) = N_A \int_0^{\infty} d\omega A(\omega, \varepsilon), \tag{7}$$

$$N_h(\varepsilon) = N_A \int_0^{\infty} d\omega A(\omega, \varepsilon + \hbar\omega). \tag{8}$$

The second expression results from the fact that for photon frequency in the range $\omega ... \omega + d\omega$ the number of created holes at energy ε is $d\omega A(\omega, \varepsilon + \hbar\omega)$, that is, equal to the number of created electrons at energy $\varepsilon + \hbar\omega$. Note that $N_e(\varepsilon)I(t)$ and $N_h(\varepsilon)I(t)$ are the rates of generating electrons and holes, respectively, and that $\int d\varepsilon N_e(\varepsilon) = \int d\varepsilon N_h(\varepsilon) = N_A$ is the number of electron-hole pairs produced by the excitation. The electronic population at energy ε can change due to absorption of a photon of energy $\hbar\omega$ not only by promoting an electron from energy $\varepsilon - \hbar\omega$, but also by promoting an electron from ε to $\varepsilon + \hbar\omega$. The net change of electronic population at energy ε per unit time and energy is $N_A I(t)\phi(\varepsilon)$, where

$$\phi(\varepsilon) \equiv \int_0^{\infty} d\omega [A(\omega, \varepsilon) - A(\omega, \varepsilon + \hbar\omega)]. \tag{9}$$

In principle, the incident radiation also affects downward transitions by induced photon emission, but we assume that such processes are negligible.

The function $\phi(\varepsilon)$ can be used to express the desired rate of change of the electronic distribution. We write the latter as

$$f(\varepsilon, t) = f_{eq}(\varepsilon, t) + f_p(\varepsilon, t), \tag{10}$$

where the time dependence of the equilibrium Fermi-Dirac distribution f_{eq} reflects the time-dependence of the particle temperature. The nonequilibrium, light-induced component in Eq. (10) is thus,

$$\dot{f}_p(\varepsilon, t) = \frac{N_A I(t)}{\rho(\varepsilon)}\phi(\varepsilon). \tag{11}$$

In what follows we make the simplifying assumption that $D(\varepsilon_e, \varepsilon_e - \omega)$ in Eq. (5) is a constant (i.e., all electronic transitions are equally probable), which can be taken to be unity without loss of generality. We also disregard the energy dependence of the electronic density of states ρ (a reasonable approximation for processes that involve electronic states near the Fermi energy[57–59]), and, for the purpose of evaluating ρ_p from Eqs. (5) and (6), assume that f can be roughly approximated by f_{eq}. This leads to

$$\rho_p(\varepsilon_e, \varepsilon_e - \hbar\omega) = \frac{\rho^2}{(e^{(\varepsilon_e - \hbar\omega)\beta_e} + 1)(e^{-\varepsilon_e\beta_e} + 1)}, \tag{12}$$

(where $\beta_e = (k_B T)^{-1}$ may be time dependent). Equations (3) and (5) (in the form $A(\omega, \varepsilon_e) = K n_I(\omega)\rho_p(\varepsilon_e, \varepsilon_e - \hbar\omega)$) then lead to

$$K = \frac{L(\omega)}{N_A \int_{-\infty}^{\infty} d\varepsilon_e \rho_p(\varepsilon_e, \varepsilon_e - \hbar\omega)}. \tag{13}$$

(As is evident from Eq. (12), the integration over ε_e in Eq. (13) can be extended, to a good approximation, to $\pm\infty$). Using Eqs. (13) and (14) in Eq. (5) we get

$$A(\omega, \varepsilon_e) = \frac{n_I(\omega)L(\omega)}{N_A}\frac{\rho_p(\varepsilon_e, \varepsilon_e - \hbar\omega)}{\int_{-\infty}^{\infty} d\varepsilon_e \rho_p(\varepsilon_e, \varepsilon_e - \hbar\omega)}, \tag{14}$$

or (see Appendix A)

$$A(\omega, \varepsilon) = \frac{n_I(\omega)L(\omega)}{N_A}\frac{1 - e^{-\hbar\omega\beta_e}}{\hbar\omega(e^{(\varepsilon - \hbar\omega)\beta_e} + 1)(e^{-\varepsilon\beta_e} + 1)}. \tag{15}$$

Normalization is ensured by the identity (4).

Next we turn to the change in electronic population, determined by Eq. (9). From Eqs. (9) and (15) it follows that (Appendix B)

$$N_A\phi(\varepsilon) = \tanh(\varepsilon\beta_e/2) \times \int_0^{\infty}\frac{d\omega}{\hbar\omega}L(\omega)n_I(\omega)\frac{\cosh(\hbar\omega\beta_e) - 1}{\cosh(\hbar\omega\beta_e) + \cosh(\varepsilon\beta_e)}, \tag{16}$$

where, because $\phi(\varepsilon)$ is an odd function, all the relevant information is contained within $\varepsilon > 0$. Physically, this reflects the symmetry of the Fermi-Dirac function with respect to the Fermi level. Henceforth, $\phi(\varepsilon)$ is defined as $-\phi(-\varepsilon)$ for all $\varepsilon < 0$.

Equation (16) can be numerically evaluated for any given frequency profile of the incident radiation and for a given plasmon absorption lineshape $L(\omega)$. Some insight can be gained by considering two extreme limits. In one limit we consider CW excitation characterized by a sharp incident frequency ω_I, i.e.,

$$n_I(\omega) = N_I\delta(\omega - \omega_I), \tag{17}$$

obtaining from Eq. (16),

$$N_A\phi(\varepsilon, \omega_I) = N_I \tanh(\varepsilon\beta_e/2)\frac{1}{\hbar\omega_I}L(\omega_I) \times \frac{\cosh(\hbar\omega_I\beta_e) - 1}{\cosh(\hbar\omega_I\beta_e) + \cosh(\varepsilon\beta_e)}. \tag{18}$$

In the common case, where $\hbar\omega_I\beta_e \gg 1$, this simplifies to

$$N_A\phi(\varepsilon, \omega_I) = \frac{N_I}{\hbar\omega_I}L(\omega_I)\frac{\tanh(\varepsilon\beta_e/2)}{1 + e^{-\beta_e\hbar\omega_I}\cosh(\varepsilon\beta_e)}. \tag{19}$$

Note that in this case $N_I L(\omega_I) = N_A$, so in fact Eq. (19) is an expression for $\phi(\varepsilon, \omega_I)$.

In the opposite limit, the incident radiation field is broadband with a flat spectrum encompassing the plasmon lineshape profile. In this case $n_I(\omega) = n_I$ does not depend on ω. Using a simple Lorenzian lineshape model, $L(\omega) = \Gamma_0^2[(\omega - \omega_0)^2 + \Gamma^2]^{-1}$ (where $(\Gamma_0/\Gamma)^2 \leq 1$ is the light absorption probability at the peak), one finds

$$\frac{N_A}{n_I}\phi(\varepsilon) = \tanh(\beta_e\varepsilon/2)\int_0^{\infty}\frac{d\omega}{\hbar\omega}\frac{\cosh(\beta_e\hbar\omega) - 1}{\cosh(\beta_e\hbar\omega) + \cosh(\beta_e\varepsilon)} \times \frac{{\Gamma_0}^2}{(\omega - \omega_0)^2 + \Gamma^2} \tag{20}$$

For typical values of the lineshape parameters, e.g., $\hbar\omega_0 = 2.5$ eV and $\hbar\Gamma = 0.3$ eV, the Lorentzian function is relatively sharply peaked about ω_0, while the function that multiplies it is relatively smooth. Furthermore, at room temperature, $\beta_e^{-1} \sim (1/40)$ eV and $\cosh(\beta_e\hbar\omega_0) \gg 1$. Equation (20) can therefore be approximated by

$$\frac{N_A}{n_I}\phi(\varepsilon) = \frac{\pi{\Gamma_0}^2}{\hbar\omega_0\Gamma}\tanh\left(\frac{\beta_e\varepsilon}{2}\right)\frac{1}{1 + 2e^{-\beta_e\hbar\omega_0}\cosh(\beta_e\varepsilon)}. \tag{21}$$

As a function of ε, this distribution starts from zero at $\varepsilon = 0$, goes through a maximum for intermediate values of ε, and vanishes as $\varepsilon \to \infty$. Figure 1 shows the form of this

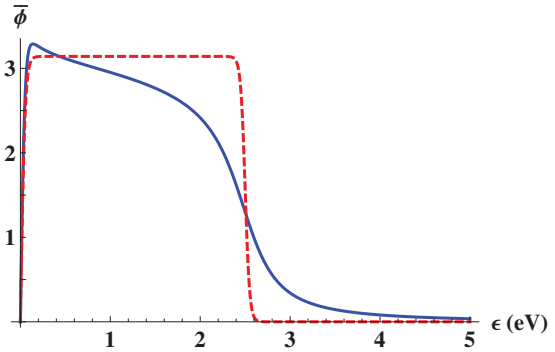

FIG. 1. The dimensionless electron-hole distribution $\bar{\phi}(\varepsilon) = \frac{\hbar\omega_0\Gamma}{\Gamma_0^2}N_A / n_I\phi(\varepsilon)$ plotted against ε, as calculated from Eq. (20) (solid curve) and from the approximation (21) (dashed curve). See text for parameters.

distribution, for the above choice of parameters, as obtained from Eq. (20) and from the approximation (21). While qualitative agreement is seen, it is seen that the approximate result is too crude for quantitative calculations. (Clearly, the agreement improves as Γ decreases.) In actual calculations for this limit it is preferable to use the exact result of Eq. (20).

III. DYNAMICS

The change in the electronic distribution arising from the excitation term (11) is counterbalanced by electron thermalization, which occurs on a sub-picosecond timescale. A rigorous model would consider electron equilibration as a scattering problem, using the Boltzmann equation and numerical integration,[59–61] for instance. In what follows we use a simpler model based on the relaxation time approximation. Under this approximation, the rate of change of the electronic distribution is described, using (11), by

$$\frac{df_p(\varepsilon,t)}{dt} = -\frac{1}{\tau_e(\varepsilon)} f_p(\varepsilon,t) + \frac{N_A I(t)}{\rho(\varepsilon)}\phi(\varepsilon,\omega_I), \tag{22}$$

where $\tau_e(\varepsilon)$ is the relaxation time of the excess distribution that may depend on the energy ε. Note that the appearance of ω_I on the rhs reflects the dependence of the resulting non-equilibrium electronic distribution on the characteristic incident frequency but should be taken to stand for all parameters that characterize the incident radiation, such as the pulse width. We note also that the function $\phi(\varepsilon,\omega_I)$ is time-dependent if the particle's temperature changes during the light pulse. In the rest of this section we consider situations where this time dependence may be disregarded; the extension to the case where the time-dependence of $\phi(\varepsilon,\omega_I)$ is non-negligible is discussed in Sec. IV.

The energy balance equation associated with Eq. (22) can be made explicit by multiplying this equation by $\varepsilon\rho(\varepsilon)$ and integrating over ε,

$$\frac{dE_p}{dt} = -\int_{-\infty}^{\infty} d\varepsilon \frac{\varepsilon\rho(\varepsilon)}{\tau_e(\varepsilon)} f_p(\varepsilon,t) + N_A I(t)\int_{-\infty}^{\infty} d\varepsilon\,\varepsilon\phi(\varepsilon). \tag{23}$$

The last term on the right-hand side can be recast in a physically transparent form, as discussed in what follows. From (9) we have that

$$\int_{-\infty}^{\infty} d\varepsilon\,\varepsilon\phi(\varepsilon) = \hbar\int_0^{\infty} d\omega\,\omega\int_{-\infty}^{\infty} d\varepsilon A(\omega,\varepsilon), \tag{24}$$

which, using (3), provides an expression for the rate of energy absorption by the electronic system,

$$N_A I(t)\int_{-\infty}^{\infty} d\varepsilon\,\varepsilon\phi(\varepsilon) = I(t)\hbar\int_0^{\infty} d\omega\,\omega n_I(\omega)L(\omega)$$
$$= \hbar\int_0^{\infty} d\omega\,\omega\dot{n}_I(\omega,t)L(\omega). \tag{25}$$

The first term on the right-hand side of Eq. (23) corresponds to the energy loss associated with the relaxation of f_p to electronic equilibrium. We will return to this energy balance in Sec. IV.

At steady state, $N_A I = \dot{N}_A =$ constant and so is the temperature. Eq. (22) with $df_p/dt = 0$ yields

$$f_p(\varepsilon,t) = \frac{\dot{N}_A\tau_e(\varepsilon)}{\rho(\varepsilon)}\phi(\varepsilon,\omega_I). \tag{26}$$

For a pulsed excitation, starting from $f_p(\varepsilon, t=0) = 0$, Eq. (22) leads to

$$f_p(\varepsilon,t) = \frac{N_A\phi(\varepsilon,\omega_I)}{\rho(\varepsilon)}\int_0^t dt' e^{-[1/\tau_e(\varepsilon)](t-t')} I(t') \tag{27}$$

In particular, for the nearly monochromatic pulse described by Eqs. (2) and (17),

$$f_p(\varepsilon,t) = \frac{L(\omega_I)}{\hbar\omega_I\rho(\varepsilon)}\frac{\tanh(\varepsilon\beta_e/2)}{1+e^{-\beta\hbar\omega_I}\cosh(\varepsilon\beta_e)}$$
$$\times\int_0^t dt' e^{-[1/\tau_e(\varepsilon)](t-t')}\dot{N}_I(t'), \tag{28}$$

where $\dot{N}_I(t) = N_I I(t)$ is the incident light intensity at time t. The corresponding steady state result is obtained by setting $\dot{N}_I =$ constant and integrating to $t\to\infty$.

Because $\int_{-\infty}^{\infty} d\varepsilon\rho(\varepsilon) f_p(\varepsilon) = 0$ and since $\phi(\varepsilon)$ is an odd function of ε, $\tau_e(\varepsilon)$ has to be an even function of ε. For the energy dependent relaxation time the model $\tau_e(\varepsilon)\sim\varepsilon^{-2}$ with a constant τ_1, has been used.[62] This model disregards the possible non-equilibrium character of secondary electron distribution generated by the scattering processes[61] and is therefore strictly valid only if the non-thermal component in the secondary electron distribution is negligible. It also neglects the metal band structure, which factors in the electron relaxation time.[63] For the calculations discussed below, however, this approximation for $\tau_e(\varepsilon)$ is adequate.

IV. ENERGY ABSORPTION AND TEMPERATURE

As discussed above, light absorption by the electronic subsystem leads to a sequence of relaxation processes. Following electronic excitation, fast dephasing leads to an excited, nonequilibrium electronic distribution $f_p(\varepsilon)$. Subsequent relaxation within the electronic subsystem results in a thermal electronic distribution $f_{eq}(\varepsilon)$—a Fermi-Dirac distribution characterized by an electronic temperature T_e. This is the process described by Eq. (22), which should be supplemented by a kinetic equation for the electronic temperature T_e. The time evolution of this temperature results from the balance between energy injection from the relaxation of $f_p(\varepsilon)$ and energy dissipation by equilibration with the underlying vibrational motion in the particle, as described by the two-temperature model.[25,26] Finally, long time evolution of the system temperature results in particle cooling by equilibration with the surrounding environment. A complete dynamical description of the temperature evolution would require augmenting Eq. (25) to include all these (for the most part–sequential) processes.

In what follows we simplify this description in order to focus on the electronic processes of interest. We assume that

the electronic system is embedded in a thermal environment with a given fixed temperature T_{env} and that the equilibration of the electronic temperature T_e with this environment is governed by a relaxation term of the form $-\kappa\,(T_e - T_{env})$ with a relaxation constant κ. This relaxation counter-balances the increase in thermal electronic energy affected by the decay of the nonequilibrium distribution $f_p(\varepsilon)$. [In principle, the relaxation of $f_p(\varepsilon)$ is also affected by coupling to the thermal environment. Our approach is based, as outlined above, on the assumption of timescale separation between the fast internal relaxation of the non-thermal electronic distribution f_p and the subsequent relaxation of the hot thermal distribution $f_{eq}^{(e)}$, that is, $\kappa \ll \langle\tau_e\rangle^{-1}$.] This contribution to the change in T_e can be calculated from the rate of increase in the energy contents of the equilibrium electronic distribution $f_{eq}^{(e)}(\varepsilon) = (e^{\beta_e(t)\varepsilon} + 1)^{-1}$, given by the first term on the right hand side of Eq. (23), that is

$$\frac{d}{dt}\int_{-\infty}^{\infty} d\varepsilon\;\varepsilon\;\rho(\varepsilon)(e^{\beta_e(t)\varepsilon}+1)^{-1} = \int_{-\infty}^{\infty} d\varepsilon\frac{\varepsilon\rho(\varepsilon)}{\tau_e(\varepsilon)}f_p(\varepsilon,t), \tag{29a}$$

or, within the approximation of an energy-independent density, $\rho(\varepsilon) = \rho$,

$$\frac{d}{dt}\int_{-\infty}^{\infty} d\varepsilon\;\varepsilon\,(e^{\beta_e(t)\varepsilon}+1)^{-1} = \int_{-\infty}^{\infty} d\varepsilon\frac{\varepsilon}{\tau_e(\varepsilon)}f_p(\varepsilon,t). \tag{29b}$$

On the left-hand side we note that the Fermi distribution is written with respect to the Fermi energy as the origin, hence ε in front of the distribution should be replaced by $\varepsilon+E_F$ (we disregard the difference between the Fermi energy and the chemical potential in this calculation). Given, however that $(d/dt)\,(e^{\beta_e(t)\varepsilon}+1)^{-1} = (d\beta_e/dt)\,(d/d\beta_e)(e^{\beta_e(t)\varepsilon}+1)^{-1}$, which is an odd function of ε, the term multiplying E_F vanishes. The additional term makes no contribution to the right hand side either because $\int_{-\infty}^{\infty} d\varepsilon\frac{\rho(\varepsilon)}{\tau_e(\varepsilon)}f_p(\varepsilon,t) = 0$. The left-hand side of (29b) may be rewritten in the form $-(c/\beta^3)\,(d\beta/dt) = ck_B{}^2TdT/dt$ where $c = \int_{-\infty}^{\infty} dx\,x^2(e^{x/2}+e^{-x/2})^{-2} = \pi^2/3$. Using this result, together with the simple relaxation model introduced above, (Eq. (29b)) leads to

$$\frac{dT_e}{dt} = \frac{3}{\pi^2k_B^2}\frac{1}{T_e}\int_{-\infty}^{\infty} d\varepsilon\frac{\varepsilon}{\tau_e(\varepsilon)}f_p(\varepsilon,t) - \kappa(T_e - T_{env}). \tag{30}$$

At steady state, $dT_e\,/\,dt = 0$, driven with light of frequency ω_I, Eqs. (19) and (26) yield,

$$\frac{3}{\pi^2k_B^2}\frac{\dot{N}_I L(\omega_I)}{\rho\hbar\omega_I}\frac{1}{T_e}\int_{-\infty}^{\infty} d\varepsilon\frac{\varepsilon\tanh(\varepsilon\beta_e/2)}{1+e^{-\beta\omega_I}\cosh(\varepsilon\beta_e)} = \kappa(T_e - T_{env}). \tag{31}$$

A simpler route to this result is to use the equality, at steady state, of the two terms on the right of Eq. (23), with which the integral in (30) is replaced by the second of these terms.

V. ELECTRON TRANSPORT

In this subsection, we proceed to apply the formulation of Sec. II to explore light-triggered transport via molecular junctions. Light can affect electronic conduction in nanojunctions in different ways, including controlled modifications in the geometry of the molecular component of the junction,[55,56] creation of dressed states with desired conductance properties,[64] local fields,[65] frequency chirps,[66] the coherent effect of a pulse sequence,[67] and destructive quantum interference,[68] to mention just a subset of the relevant recent literature.[69] Here we focus on one of the variety of possible optically induced phenomena, namely, the effect of the electronic non-equilibrium induced by plasmonic light absorption. We consider the Landauer theory expression for the current

$$I = \frac{e}{\pi\hbar}\int_{-\infty}^{\infty} d\varepsilon[f_1(\varepsilon) - f_2(\varepsilon)]\mathcal{T}(\varepsilon), \tag{32}$$

where e is the electron charge, $f_j(\varepsilon)$ $(j = 1,2)$ is the electronic distribution in electrode j and $\mathcal{T}(\varepsilon)$ is the transmission function at electron energy ε, and assume that nonequilibrium between the electrodes results from the fact that one of them, say electrode 1, is illuminated. From Eq. (10), $f_1(\varepsilon,t) - f_2(\varepsilon) = f_{eq}^{(1)}(\varepsilon,t) - f_{eq}^{(2)}(\varepsilon) + f_p^{(1)}(\varepsilon,t)$. The difference $f_{eq}^{(1)}(\varepsilon,t) - f_{eq}^{(2)}(\varepsilon)$, which reflects the different electronic temperatures of two electrodes created by the illumination, will give rise to thermoelectric response that can be analyzed by standard methods. Our interest here is in the additional effect associated with the generation of the nonequilibrium electronic distribution $f_p^{(1)}(\varepsilon)$. This nonequilibrium component can be a short time transient following a pulse excitation or a time independent addition to the electronic distribution in the case of continuous illumination. To explore the role played by the nonequilibrium electron distribution established by the light on the transport properties, we focus on the current associated with $f_p^{(1)}(\varepsilon)$, (the superscript (1) will be dropped henceforth), denoted I_p in what follows. This corresponds to the situation where only one electrode is illuminated, or where one electrode relaxes to the electronic thermal distribution much faster than the other, and therefore provides an upper limit to this contribution. In the case of constant illumination with light of frequency ω_I, Eqs. (32), (26), and (19) lead to

$$I_p = \frac{e}{\pi\hbar}\frac{\dot{N}_I}{\hbar\omega_I}L(\omega_I)\int_{-\infty}^{\infty} d\varepsilon\frac{\tau_e(\varepsilon)}{\rho(\varepsilon)}\frac{\tanh(\varepsilon\beta_e/2)}{1+e^{-\beta_e\hbar\omega_I}\cosh(\varepsilon\beta_e)}\mathcal{T}(\varepsilon). \tag{33}$$

Consider the simplest junction model, where transmission is dominated by a single conduction resonance, $\mathcal{T}(\varepsilon) = \Gamma_1\Gamma_2[(\varepsilon-\varepsilon_0)^2 + (1/4)\,(\Gamma_1+\Gamma_2)^2]^{-1}$, characterized by the resonance energy ε_0 and the resonance widths Γ_1, Γ_2 associated with decay of the resonance into the two electrodes. If these widths are small with respect to $\varepsilon-\varepsilon_0$, Eq. (33) can be approximated by

$$I_p \cong \frac{e}{\hbar}\frac{\dot{N}_I}{\hbar\omega_I}L(\omega_I)\frac{\tau_e(\varepsilon_0)}{\rho(\varepsilon_0)}\frac{1}{1+(1/2)e^{\beta_e(\varepsilon_0-\hbar\omega_I)}}\frac{\Gamma_1\Gamma_2}{(\Gamma_1+\Gamma_2)}, \tag{34}$$

where we have assumed that $\varepsilon_0\beta_e \gg 1$. Note that the current direction depends on whether the dominant carriers are electrons or holes. As in the approximation (21) to Eq. (20), Eq. (34) should be regarded as a tool for qualitative discussions or rough estimates.

Alternatively we may focus on the photovoltage response—the voltage needed to make this current component zero. Anticipating that this voltage will be in the linear regime, it satisfies

$$I_p = -(e^2/\pi\hbar)\mathcal{T}(\varepsilon = 0)V_p, \tag{35}$$

and its sign again depends on the nature of the charge carriers.

To estimate this contribution to the light induced current, we start by assuming a weak CW laser intensity of 1 W/cm^2. With 10^{19} surface atoms per m^2, this translates into 10^{-15} W/atom. Taking $\omega_I = 3$ eV, this amounts to $\dot{N}_I = 2*10^3$ photons per sec per atom.

Using a free electron model with electron effective mass 1 a.u., the density of states per atom is of the order $\rho(\varepsilon) \sim 10^{-1}$ eV^{-1} at $\varepsilon = 3$ eV. Taking also $\tau_e = 10^{-14}$ s, $L(\omega_I) = 1$ (the latter choice amounts to assuming that all photons are absorbed, in the spirit of looking for an upper bound) and $\Gamma_1\Gamma_2/(\Gamma_1 + \Gamma_2) = 0.1$ eV, Eq. (34) yields $I_p/e \sim 1.01 \times 10^4$ s^{-1} while using Eq. (33) we can get $I_p/e = 1.25 \times 10^4$ s^{-1} as the maximum current at $\Gamma_2 = 0.2$ eV. This number appears small, but can become substantial because of several factors. First, considering a tip-surface configuration as a convenient nanojunction structure, the number of surface atoms contributing to the current will usually be larger than 1. Second, in such configurations plasmonic enhancement of the local field at the junction can lead to a signal larger by several (3-4) orders of magnitudes. Finally, larger incident intensities can be used without jeopardizing the stability of the system; see, for example, Ref. 70, where an incident intensity of ~560 W/cm^2 was used in a tip-enhanced Raman measurement (and an intensity enhancement of 3 orders of magnitude was observed). Clearly, much higher intensities can be applied with pulsed sources. Under such conditions, the estimated current readily reaches observable magnitudes, of order $I_p/e \sim 10^{11}$ s^{-1} or $I_p \sim 10$ nA. It should be noted that the steady state excess (due to illumination) current obtained from this mechanism is superimposed on a thermoelectric signal associated with the different electronic temperatures transiently developed on the two electrodes. These different contributions can, in principle, be distinguished by the different timescales on which they relax.

VI. CONCLUSIONS

We have examined the properties of the non-equilibrium electronic distribution created in a metal nanoparticle as a result of light absorption. This distribution results from the fast decoherence of the initially formed plasmon, and reflects the balance between this decoherence process and subsequent thermalization processes. We have distinguished between the electronic non-equilibrium that expresses itself as deviation from a Fermi-Dirac distribution and relaxes on the ~10 fs timescale, and the subsequently established electronic equilibrium at an electronic temperature higher than the ambient temperature, which relaxes on much slower timescales, and have focused on the former. Our approach, aimed to enable qualitative insights and rough estimates, is based on simple free electron modeling of the metal particle.

Our calculation entails several approximations that make our results mainly of qualitative value. First, it is based on a free electron model that may be insufficient for quantitative calculations of electron dynamics in metal nanoparticles. In the same spirit, interband contribution to the electronic response was disregarded, an approximation justified for silver at the spectral regimes studied, but not for gold. Finally, for particles that are not very small, the timescale separation assumed for relaxation due to e-e scattering and that resulting from electron phonon coupling is not very sharp, and both processes may contribute to the relaxation time τ_e in Eqs. (33) and (34). (This fact will not affect the results within the simple model through which they were derived.) A quantitative study should address these issues.

Effects of the non-thermal nature of the electronic distribution following plasmon absorption can be manifested under steady state conditions, as exemplified by observations of plasmon enhanced photoemission, see, e.g., Ref. 71. The timescale associated with the plasmon decoherence and the subsequent relaxation of the non-equilibrium electronic distribution can be monitored using two-photon photoemission,[72] ultrafast non-linear response,[52,73–76] hole-burning spectroscopy,[77] or the core hole clock technique,[78] for instance. Here we have considered another possible steady state consequence, and have estimated the magnitude of the electronic current that can be generated in an illuminated plasmonic nanojunction in which the two electrodes are exposed to different light intensities or at least respond differently to the incoming light, as expected to be the case in typical tip-surface junctions. We have found that under favorable conditions of light intensity and asymmetry, measurable currents can be generated. It will be interesting to explore similar effects in photochemical processes on metal particles that are initiated by light-triggered plasmon excitation in the particle. This and other applications will be the topics of future research.

ACKNOWLEDGMENTS

T.S. is grateful to the U.S. National Science Foundation (NSF) (Grant No. CHE-1012207/001) and the U.S. Department of Energy (DOE) (Grant No. DE-SC0001785) for support. T.S. and A.N. thank the United States-Israel Binational Science Foundation (Grant No. 2008124), A.N. thanks the European Research Council under the European Union's Seventh Framework Program, FP7/2007-2013; ERC Grant Agreement No. 22662, and the Israel Science Foundation. M.K. thanks the National Science Foundation's MRSEC program (DMR-1121262) at the Materials Research Center of Northwestern University for a Research Experience for Undergraduate Students (REU) summer fellowship.

APPENDIX A: DERIVATION OF EQ. (15)

From (12)

$$\frac{\rho_p(\varepsilon,\varepsilon-\hbar\omega)}{\int_{-\infty}^{\infty} d\varepsilon \rho_p(\varepsilon,\varepsilon-\hbar\omega)} = \frac{1}{(e^{(\varepsilon-\hbar\omega)\beta_e}+1)(e^{-\varepsilon\beta_e}+1)} \times \left[\int_{-\infty}^{\infty} d\varepsilon \frac{1}{e^{(\varepsilon-\hbar\omega)\beta_e}+1}\frac{1}{e^{-\varepsilon\beta_e}+1}\right]^{-1}. \quad \text{(A1)}$$

The integral in (A1) can be evaluated analytically, yielding

$$\int_{-\infty}^{\infty} d\varepsilon_e \frac{1}{e^{(\varepsilon_e-\hbar\omega)\beta_e}+1}\frac{1}{e^{-\varepsilon_e\beta_e}+1} = \frac{1}{\beta_e}\frac{1}{1-e^{-\beta_e\hbar\omega}}\int_{-\infty}^{\infty} d\varepsilon_e\left(\frac{1}{1+e^{\beta_e(\varepsilon_e-\hbar\omega)}}-\frac{1}{1+e^{\beta_e\varepsilon_e}}\right) = \frac{\hbar\omega}{1-e^{-\beta_e\hbar\omega}}. \quad \text{(A2)}$$

This leads to Eq. (15).

APPENDIX B: DERIVATION OF EQ. (16)

$$\hbar N_A\phi(\varepsilon) = \int_0^{\infty} d\omega \frac{L(\omega)n_I(\omega)(1-e^{-\beta_e\hbar\omega})}{\hbar\omega}\left[\frac{1}{(1+e^{\beta_e(\varepsilon-\hbar\omega)})(1+e^{-\beta_e\varepsilon})}-\frac{1}{(1+e^{\beta_e\varepsilon})(1+e^{-\beta_e(\varepsilon+\hbar\omega)})}\right]$$

$$= \int_0^{\infty} d\omega \frac{L(\omega)n_I(\omega)(1-e^{-\beta_e\hbar\omega})}{\hbar\omega(e^{(1/2)\beta_e\varepsilon}+e^{-(1/2)\beta_e\varepsilon})}\left[\frac{e^{(1/2)\beta_e\varepsilon}}{1+e^{\beta_e(\varepsilon-\hbar\omega)}}-\frac{e^{-(1/2)\beta_e\varepsilon}}{1+e^{-\beta_e(\varepsilon+\hbar\omega)}}\right]$$

$$= \int_0^{\infty} d\omega \frac{L(\omega)n_I(\omega)(1-e^{-\beta_e\hbar\omega})}{\hbar\omega(e^{(1/2)\beta_e\varepsilon}+e^{-(1/2)\beta_e\varepsilon})}\left[\frac{e^{(1/2)\beta_e\varepsilon}-e^{-(1/2)\beta_e\varepsilon}+e^{-\beta_e((1/2)\varepsilon+\hbar\omega)}-e^{\beta_e((1/2)\varepsilon-\hbar\omega)}}{e^{-2\beta_e\hbar\omega}+1+e^{\beta_e(\varepsilon-\omega\hbar)}+e^{-\beta_e(\varepsilon+\hbar\omega)}}\right]$$

$$= \int_0^{\infty} d\omega \frac{L(\omega)n_I(\omega)(1-e^{-\beta\hbar\omega})}{\hbar\omega(e^{(1/2)\beta_e\varepsilon}+e^{-(1/2)\beta_e\varepsilon})}\left[\frac{(e^{(1/2)\beta_e\varepsilon}-e^{-(1/2)\beta_e\varepsilon})(1-e^{-\beta_e\hbar\omega})}{e^{-\beta_e\hbar\omega}(e^{-\beta_e\hbar\omega}+e^{\beta_e\hbar\omega}+e^{\beta_e\varepsilon}+e^{-\beta_e\varepsilon})}\right]$$

$$= \int_0^{\infty} d\omega \frac{L(\omega)n_I(\omega)(e^{(1/2)\beta_e\varepsilon}-e^{-(1/2)\beta_e\varepsilon})}{\hbar\omega(e^{(1/2)\beta_e\varepsilon}+e^{-(1/2)\beta_e\varepsilon})}\frac{(e^{\beta_e\hbar\omega}+e^{-\beta_e\hbar\omega}-2)}{(e^{-\beta_e\hbar\omega}+e^{\beta_e\hbar\omega}+e^{\beta_e\varepsilon}+e^{-\beta_e\varepsilon})}$$

[1] L. Cao, D. N. Barsic, A. R. Guichard, and M. L. Brongersma, Nano Lett. **7**, 3523–3527 (2007).
[2] H. M. Pollock and A. Hammiche, J. Phys. D **34**, R23–R53 (2001).
[3] W. A. Challener, C. Peng, A. V. Itagi, D. Karns, W. Peng, Y. Peng, X. Yang, X. Zhu, N. J. Gokemeijer, Y. T. Hsia, G. Ju, R. E. Rottmayer, M. A. Seigler, and E. C. Gage, Nat. Photonics **3**, 220–224 (2009).
[4] V. Garces-Chavez, R. Quidant, P. J. Reece, G. Badenes, L. Torner, and K. Dholakia, Phys. Rev. B **73**, 085417 (2006).
[5] G. L. Liu, J. Kim, Y. Lu, and L. P. Lee, Nature Mater. **5**, 27–32 (2006).
[6] X. Miao, B. K. Wilson, and L. Y. Lin, Appl. Phys. Lett. **92**, 124108 (2008).
[7] D. Ross, M. Gaitan, and L. E. Locascio, Anal. Chem. **73**, 4117–4123 (2001).
[8] S. Lal, S. E. Clare, and N. J. Halas, Acc. Chem. Res. **41**, 1842–1851 (2008).
[9] L. Wang and B. Li, Phys. Rev. Lett. **99**, 177208 (2007).
[10] A. M. Gobin, M. H. Lee, N. J. Halas, W. D. James, R. A. Drezek, and J. L. West, Nano Lett. **7**, 1929–1934 (2007).
[11] G. Han, P. Ghosh, M. De, and V. Rotello, NanoBiotechnology **3**, 40–45 (2007).
[12] P. K. Jain, I. H. El-Sayed, and M. A. El-Sayed, Nanotoday **2**, 18–29 (2007).
[13] D. Pissuwan, S. M. Valenzuela, and M. B. Cortie, Trends Biotechnol. **24**, 62–67 (2006).
[14] A. G. Skirtach, C. Dejugnat, D. Braun, A. S. Susha, A. L. Rogach, W. J. Parak, H. Mohwald, and G. B. Sukhorukov, Nano Lett. **5**, 1371–1377 (2005).
[15] W. Zhao and J. M. Karp, Nature Mater. **8**, 453–454 (2009).
[16] G. Baffou, M. P. Kreuzer, F. Kulzer, and R. Quidant, Opt. Express **17**, 3291–3298 (2009).
[17] S. Berciaud, D. Lasne, G. A. Blab, L. Cognet, and B. Lounis, Phys. Rev. B **73**, 045424 (2006).
[18] D. Boyer, P. Tamarat, A. Maali, B. Lounis, and M. Orrit, Science **297**, 1160–1163 (2002).
[19] D. Lasne, G. A. Blab, S. Berciaud, M. Heine, L. Groc, D. Choquet, L. Cognet, and B. Lounis, Biophys. J. **91**, 4598–4604 (2006).
[20] L. Wang and B. Li, Phys. Rev. Lett. **101**, 267203 (2008).
[21] C. W. Chang, D. Okawa, A. Majumdar, and A. Zettl, Science **314**, 1121–1124 (2006).
[22] N. Yang, G. Zhang, and B. Li, Appl. Phys. Lett. **93**, 243111 (2008).
[23] M. Hu, C. Novo, A. Funston, H. Wang, H. Staleva, S. Zou, P. Mulvaney, Y. Xia, and G. V. Hartland, J. Mater. Chem. **18**, 1949–1960 (2008).
[24] U. Kreibig and M. Vollmer, *Optical Properties of Metal Clusters* (Springer, Berlin/New York, 1995).
[25] M. I. Kaganov, I. M. Lifshitz, and L. V. Tanatarov, Sov. Phys. JETP-USSR **4**, 173–178 (1957).
[26] S. I. Anisimov, B. L. Kapeliov, and T. L. Perelman, Zh. Eksp. Teor. Fiz. **66**, 776–781 (1974).
[27] M. Z. Liu and P. Guyot-Sionnest, J. Phys. Chem. B **108**, 5882–5888 (2004).
[28] C. Novo, D. Gomez, J. Perez-Juste, Z. Zhang, H. Petrova, M. Reismann, P. Mulvaney, and G. V. Hartland, Phys. Chem. Chem. Phys. **8**, 3540–3546 (2006).

[29]C. Sonnichsen, T. Franzl, T. Wilk, G. von Plessen, J. Feldmann, O. Wilson, and P. Mulvaney, Phys. Rev. Lett. **88**, 077402 (2002).
[30]T. S. Ahmadi, S. L. Logunov, and M. A. ElSayed, J. Phys. Chem. **100**, 8053–8056 (1996).
[31]J. Y. Bigot, J. C. Merle, O. Cregut, and A. Daunois, Phys. Rev. Lett. **75**, 4702–4705 (1995).
[32]T. Tokizaki, A. Nakamura, S. Kaneko, K. Uchida, S. Omi, H. Tanji, and Y. Asahara, Appl. Phys. Lett. **65**, 941–943 (1994).
[33]N. Del Fatti, C. Voisin, F. Chevy, F. Vallee, and C. Flytzanis, J. Chem. Phys. **110**, 11484–11487 (1999).
[34]J. H. Hodak, I. Martini, and G. V. Hartland, J. Chem. Phys. **108**, 9210–9213 (1998).
[35]M. Nisoli, S. DeSilvestri, A. Cavalleri, A. M. Malvezzi, A. Stella, G. Lanzani, P. Cheyssac, and R. Kofman, Phys. Rev. B **55**, 13424–13427 (1997).
[36]S. Link, D. J. Hathcock, B. Nikoobakht, and M. A. El-Sayed, Adv. Mater. (Weinheim, Ger.) **15**, 393–396 (2003).
[37]M. B. Mohamed, V. Volkov, S. Link, and M. A. El-Sayed, Chem. Phys. Lett. **317**, 517–523 (2000).
[38]A. Plech, S. Kurbitz, K. J. Berg, H. Graener, G. Berg, S. Gresillon, M. Kaempfe, J. Feldmann, M. Wulff, and G. von Plessen, Europhys. Lett. **61**, 762–768 (2003).
[39]S. Link and M. A. El-Sayed, Int. Rev. Phys. Chem. **19**, 409–453 (2000).
[40]G. V. Hartland, Chem. Rev. (Washington, D.C.) **111**, 3858–3887 (2011).
[41]V. K. Pustovalov, Chem. Phys. **308**, 103–108 (2005).
[42]A. O. Govorov, W. Zhang, T. Skeini, H. Richardson, J. Lee, and N. A. Kotov, Nanoscale Res. Lett. **1**, 84–90 (2006).
[43]P. Keblinski, D. G. Cahill, A. Bodapati, C. R. Sullivan, and T. A. Taton, J. Appl. Phys. **100**, 054305 (2006).
[44]H. Goldenberg and C. J. Tranter, Br. J. Appl. Phys. **3**, 296–298 (1952).
[45]S. Bruzzone and M. Malvaldi, J. Phys. Chem. C **113**, 15805–15810 (2009).
[46]G. Baffou, R. Quidant, and C. Girard, Phys. Rev. B **82**, 165424 (2010).
[47]G. Baffou, R. Quidant, and F. Javier Garcia de Abajo, ACS Nano **4**, 709–716 (2010).
[48]G. Baffou, C. Girard, and R. Quidant, Phys. Rev. Lett. **104**, 136805 (2010).
[49]J. R. Cole, N. A. Mirin, M. W. Knight, G. P. Goodrich, and N. J. Halas, J. Phys. Chem. C **113**, 12090–12094 (2009).
[50]H. H. Richardson, M. T. Carlson, P. J. Tandler, P. Hernandez, and A. O. Govorov, Nano Lett. **9**, 1139–1146 (2009).
[51]N. N. Nedyalkov, S. E. Imamova, P. A. Atanasov, T. Miyanishi, and M. Obara, J. Optoelectron. Adv. Mater. **12**, 484–490 (2010).
[52]C. Voisin, N. Del Fatti, D. Christofilos, and F. Vallée, J. Phys. Chem. B **105**, 2264–2280 (2001).
[53]L. Brus, Acc. Chem. Res. **41**, 1742–1749 (2008).
[54]P. V. Kamat, J. Phys. Chem. B **106**, 7729–7744 (2002).
[55]M. G. Reuter, M. A. Ratner, and T. Seideman, Phys. Rev. A **86**, 013426 (2012).
[56]M. G. Reuter, M. Sukharev, and T. Seideman, Phys. Rev. Lett. **101**, 208303 (2008).
[57]N. E. Christensen and B. O. Seraphin, Phys. Rev. B: Condens. Matter **4**, 3321–3344 (1971).
[58]N. V. Smith, Phys. Rev. B **3**, 1862–1878 (1971).
[59]C. K. Sun, F. Vallee, L. H. Acioli, E. P. Ippen, and J. G. Fujimoto, Phys. Rev. B **50**, 15337–15348 (1994).
[60]P. Grua, J. P. Morreeuw, H. Bercegol, G. Jonusauskas, and F. Vallee, Phys. Rev. B **68**, 035424 (2003).
[61]B. Rethfeld, A. Kaiser, M. Vicanek, and G. Simon, Phys. Rev. B **65**, 214303 (2002).
[62]L. D. Pietanza, G. Colonna, S. Longo, and M. Capitelli, Eur. Phys. J. D **45**, 369–389 (2007).
[63]I. Campillo, V. M. Silkin, J. M. Pitarke, E. V. Chulkov, A. Rubio, and P. M. Echenique, Phys. Rev. B **61**, 13484–13492 (2000).
[64]B. D. Fainberg and T. Seideman, Phys. Stat. Solidi A **209**, 2433–2436 (2012).
[65]B. D. Fainberg, M. Sukharev, T.-H. Park, and M. Galperin, Phys. Rev. B **83**, 205425 (2011).
[66]B. D. Fainberg, M. Jouravlev, and A. Nitzan, Phys. Rev. B **76**, 245329 (2007).
[67]R. Saha and V. S. Batista, J. Phys. Chem. B **115**, 5234–5242 (2011).
[68]U. Kleinekathöfer, G. Li, S. Welack, and M. Schreiber, Europhys. Lett. **75**, 139–145 (2006).
[69]M. Galperin and A. Nitzan, Phys. Chem. Chem. Phys. **14**, 9421–9438 (2012).
[70]N. Jiang, E. T. Foley, J. M. Klingsporn, M. D. Sonntag, N. A. Valley, J. A. Dieringer, T. Seideman, G. C. Schatz, M. C. Hersam, and R. P. Van Duyne, Nano Lett. **12**, 5061–5067 (2012).
[71]A. Grubisic, E. Ringe, C. M. Cobley, Y. Xia, L. D. Marks, R. P. Van Duyne, and D. J. Nesbitt, Nano Lett. **12**, 4823–4829 (2012).
[72]C. D. Lindstrom and X. Y. Zhu, Chem. Rev. (Washington, D.C.) **106**, 4281–4300 (2006).
[73]B. Lamprecht, J. R. Krenn, A. Leitner, and F. R. Aussenegg, Phys. Rev. Lett. **83**, 4421–4424 (1999).
[74]B. Lamprecht, J. R. Krenn, A. Leitner, and F. R. Aussenegg, Appl. Phys. B: Lasers Opt. **69**, 223–227 (1999).
[75]B. Lamprecht, A. Leitner, and F. R. Aussenegg, Appl. Phys. B: Lasers Opt. **68**, 419–423 (1999).
[76]B. Lamprecht, A. Leitner, and F. R. Aussenegg, Appl. Phys. B: Lasers Opt. **64**, 269–272 (1997).
[77]F. Stietz, J. Bosbach, T. Wenzel, T. Vartanyan, A. Goldmann, and F. Träger, Phys. Rev. Lett. **84**, 5644–5647 (2000).
[78]L. Wang, W. Chen, and A. T. S. Wee, Surf. Sci. Rep. **63**, 465–486 (2008).